SCC Publishing
Michelets vei 8 B
1366 Lysaker Norway

ISSN: 2703-9072

Correspondence:
valentina.zharkova@northumbria.ac.uk

Vol. 6.2 (2026)
pp. 50-61

Modern Grand Solar Minimum (2020-2053)

Little Ice Age started

Valentina Zharkova [1,2]

1 - ZVS Research Enterprise Ltd., London, UK; 2 – Northumbria University, Newcastle, UK

Abstract

The two Principal Components (eigen vectors) derived with Principal Component Analysis from the solar background magnetic field defining two largest magnetic waves of the poloidal field of the Sun are shown to be generated in two layers by the solar dynamo with the dipole magnetic sources. The two magnetic waves revealed a noticeable phase shift between them resulting in the variations of 11-year cycle amplitudes in the summary curve modulated by the envelope curve with a period of 330-380 years defined by the usual wave interference with a small phase shift. This envelope curve defines the grand solar cycles separated by grand solar minima (GSMs), similar to those observed in the past: Maunder, Wolf, Oort and other grand minima. There are the two modern GSMs approaching: GSM1 (2020-2053) and GSM2 (2375-2410). During a GSM a reduction of solar irradiance is expected by about 3 W/m^2 from the modern level that causes a decrease of the average terrestrial temperature by about 1.0C. This temperature reduction is already observed for the GSM1 clearly in the Northern hemisphere from the West to East signalling the arrival of *Little Ice Age* for GSM1.

Keywords: Sun: magnetic field; sun: solar activity; sun: double dynamo; grand solar minimum; little ice age

Submitted 2026-01-30, Accepted 2026-02-20, https://doi.org/10.53234/scc202603/24

1.Introduction

1.1 Solar background magnetic field

Solar background magnetic field (SBMF) plays the essential role in dynamics of the Sun and the whole solar system by expanding the interplanetary space, forming *Parker's spiral* Parker, 1958) and *Heliospheric Current Sheet* (HCS) (Smith, 2001), while interacting with the planetary magnetic fields defining some planetary patterns. There are daily observations of solar magnetic field by Wilcox Solar Observatory (Stanford, US) with full disk magnetograms with lower spatial resolution that excludes strong magnetic fields of sunspots providing daily synoptic magnetic maps of SBMT, the surface SBMF represents a summary of all the magnetic waves generated by the Sun's background magnetic field, which reach the solar surface (photosphere).

1.2 Natural frequencies

It is well known that any system has its own unique oscillations on *natural frequencies*[4] which need to be known and considered in any future exploitation of the system. Natural frequency, measured in terms of *eigenfrequency*, is the rate at which an oscillatory system tends to oscillate in the absence of disturbance. Here are the two cases when the *natural*

frequencies were ignored which led a) in 1940 to the collapse of Tahoma bridge, US

(https://en.wikipedia.org/wiki/Tacoma_Narrows_Bridge_(1940) caused by a strong gale inducing the bridge vibration on its natural frequency or b) in 2001 to the uncontrolled swinging of the Millennial bridge in London, UK, (https://www.engr.psu.edu/ae/thesis/failures/MKP/failures/failures.wikispaces.com/Millennium_Bridge_Performance_Issues.html) oscillating on its natural torsional frequency induced by walking people.

1.3 Relevance to solar activity

Our understanding of solar activity is tested by the accuracy of its prediction. The latter became very difficult to derive from the observed sunspot numbers and to fit sufficiently close into a few 11-year cycles or even into a single cycle until it is well progressed. In addition to sunspots for the current index of solar activity with averaged sunspot numbers (SSN) and considered as proxies of a strong (toroidal) magnetic field of the Sun, we used a weak solar background (poloidal) magnetic field (SBMF) captured by the Wilcox Solar Observatory in cycles 21-23 (Hoeksema, 1984).

2. Natural frequencies, or eigen vectors, of SBMF

Natural frequencies (*eigen values*) of magnetic waves (*eigen vectors)* on the Sun's surface measured from the magnetograms of SBMF can be found by applying Principal Component Analysis (PCA) (*Jolliffe, I. T. (2002).* and calculating two Principal Components, or eigen vectors (EVs) shown in Fig.1 from the historic daily magnetic synoptic maps of the Wilcox Solar Observatory (Stanford, US) for cycles 21-23 (Shepherd et al, 2014; Zharkova et al, 2015) confirmed later for cycles 21-24 (Zharkova and Shepherd, 2022).

The authors discovered that there are two principal components, or EVs, of SBMF with close but not equal eigen values and another three pairs with smaller but the significant eigen values. The pairing denotes that the solar magnetic waves are generated in the two layers of the Sun. The PCA helps to separate magnetic waves into significant eigen vectors of wave components with given eigen values defined by the data variance. The first two eigen vectors, were representing the 39 % of the magnetic data variance, the next pair of eigen vectors covers 18 % of data variance, and the next pair of eigen vectors covers 9% of the data variance.

This pairing of magnetic waves allowed the authors (Shepherd et al, 2014; Zharkova et al., 2015) to derive the mathematical expressions for these two PCs as a function of time enabling the prediction of these EVs forward for cycles 24-26 (Fig.1).

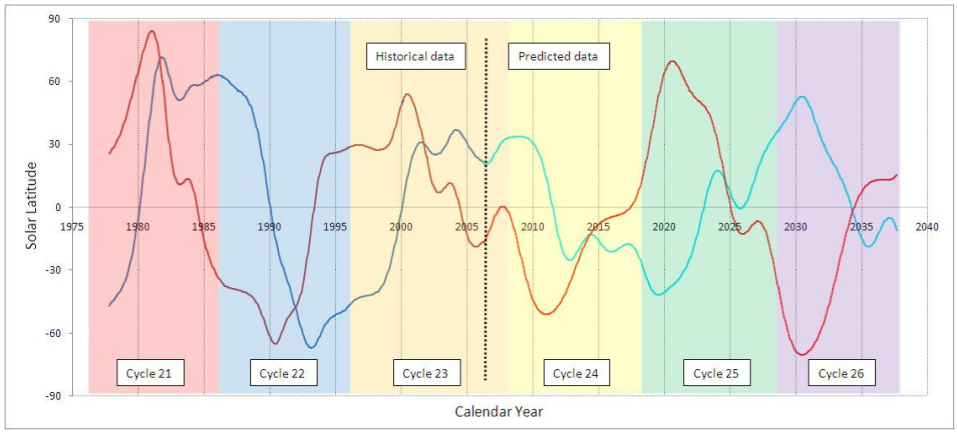

Fig.1. Two eigen vectors, or magnetic waves, derived from the solar background magnetic field with PCA in cycles 21-23 and expanded with the formula to cycles 24-26. Positive numbers indicate the northern

polarity of magnetic field and negative one - the southern polarity.

Hence, the first two PCs, or EVs, derived from PCA, shown in Fig.1, reflect the two primary magnetic waves with the different magnetic polarities (northern for positive numbers of axis Y and southern for negative ones).

In order to understand the physical meaning of the derived EVs, Zharkova et al. (2015) calculated the *summary curve* of these two EVs (Fig.2) and their *modulus summary curve* (Fig.3) reflecting all negative EVs into the positives.

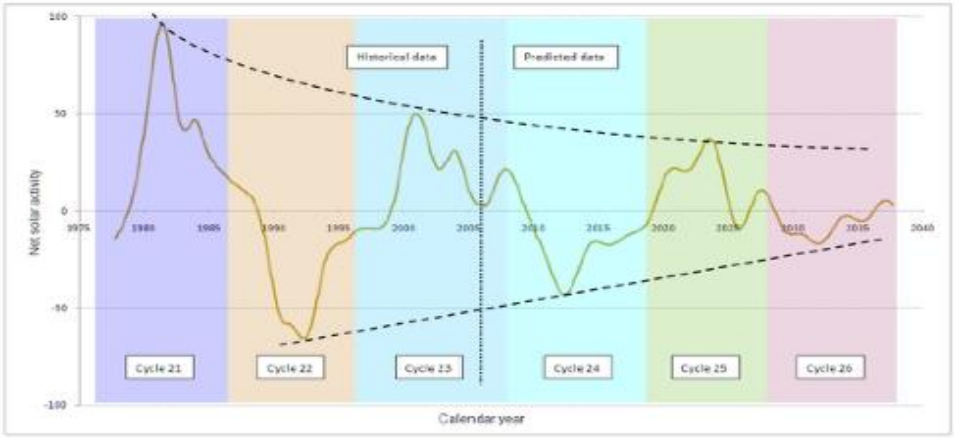

Fig.2. Summary curve of two PCs, or magnetic dynamo waves, produced by dipole magnetic sources for cycles 21-26. Positive numbers indicate the northern polarity of the summary curve and negative one – the southern polarity.

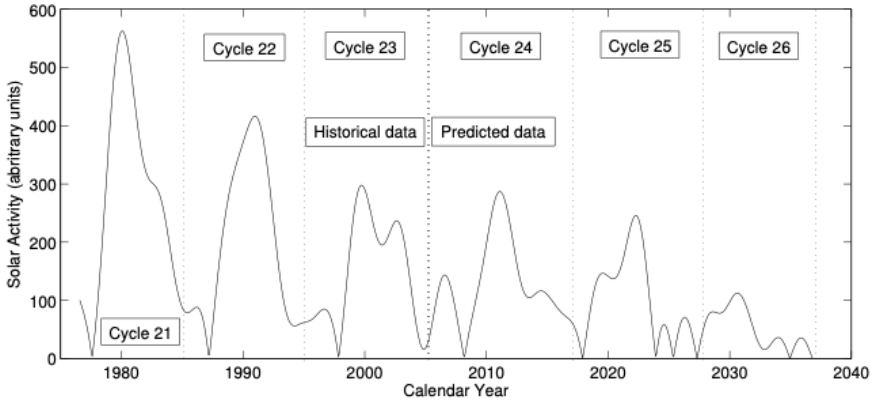

Fig.3. Modulus summary curve (mirroring the negative numbers of the summary curve in Fig.2 to the positive axis Y) of two PCs reflecting the dipole magnetic waves for cycles 21-26 showing a significant reduction of the cycle amplitude towards cycle 26.

The *Summary curve* in Fig.2 shows continuous reduction of the resulting EV magnitudes of SBMF clearly seen in Fig.3 when these magnitudes were reflected to the positive numbers only.

Hence, the *physical meaning of the natural frequencies* of the SBMF is defined by the action of solar dynamo (Cameron et al, 2017) the intrinsic source of solar activity. Keeping in mind that the solar background magnetic field (SBMF) represents poloidal magnetic field (like ocean waters) while the sunspots are considered to be proxies of the toroidal magnetic field (or magnetic

loops, like boats appearing on the surface), it makes these two types of magnetic waves (poloidal and toroidal) as the two necessary components of solar dynamo defining solar activity. Each of these types of magnetic waves is still generated in the two layers of the solar interior presenting their superposition on the surface as SBMF (poloidal field) and magnetic loops (toroidal field) with the places where they are embedded into the photosphere seen as sunspots (proxies of toroidal field).

The poloidal and toroidal magnetic waves generated by the Sun are well anti-correlated during solar cycle (Stix, 1996; Zharkov et al, 2008) confirming the dynamo process as the solar activity driver converting one type of the magnetic waves into another.

3. Summary and modulus summary curves as a complimentary solar activity index

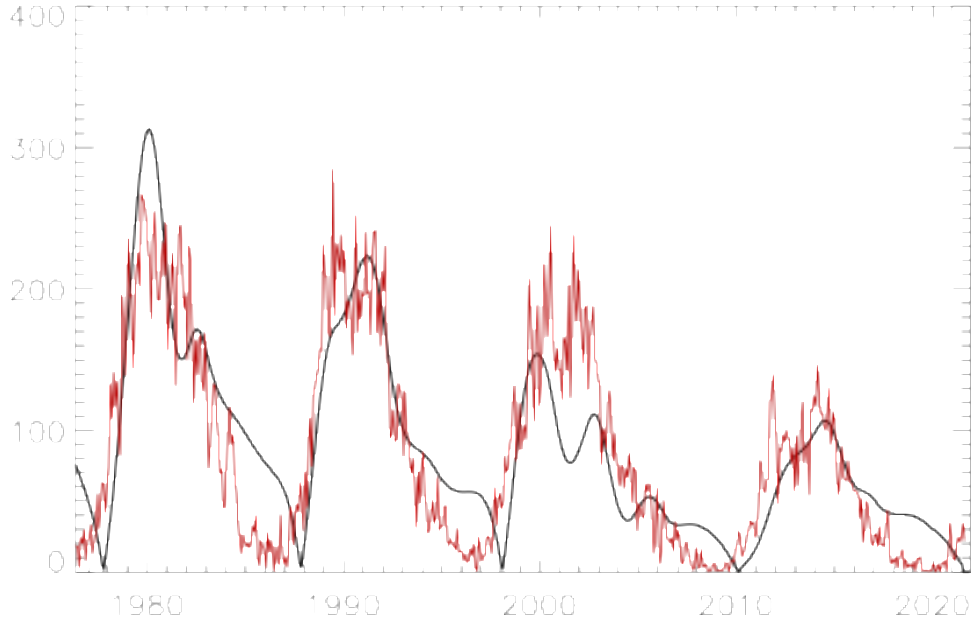

Fig.4. Comparison of the modulus summary curve with the sunspot numbers for cycles 21-24. Courtesy of Zharkova and Shepherd, 2022.

Comparison of the *modulus summary curve* (MSC) of two EVs of SBMF with the current solar activity index, averaged sunspot numbers[14] for cycles 21-24 shown in Fig.4. We showed that the sunspot activity is associated with the modulus summary curve, which is a derivative from these two-wave summary curve and not from a single one (Zharkova et al, 2015, Zharkova and Shepherd, 2022). It can be seen that the MSC of two EVs, or the waves induced by a dipole magnetic field, roughly reproduce the averaged sunspot numbers used as the current solar activity index intuitively introduced by Wolf nearly two centuries ago (Wolf, 1852).

There is more rigorous comparison of the *modulus summary curve* (MSC) with the averaged sunspot numbers (SSN) in cycles 1-25 as shown in Fig.5 (Zharkova et al, 2015). Since these two indices, MSC and SSN, represent the different entities of solar activity, respectively: magnetic waves of the background (poloidal) and sunspot (toroidal) magnetic fields of the Sun, they are not identical but complimentary by default as shown below according to the dynamo models (Zharkova, 2015, Zharkova et al, 2023).

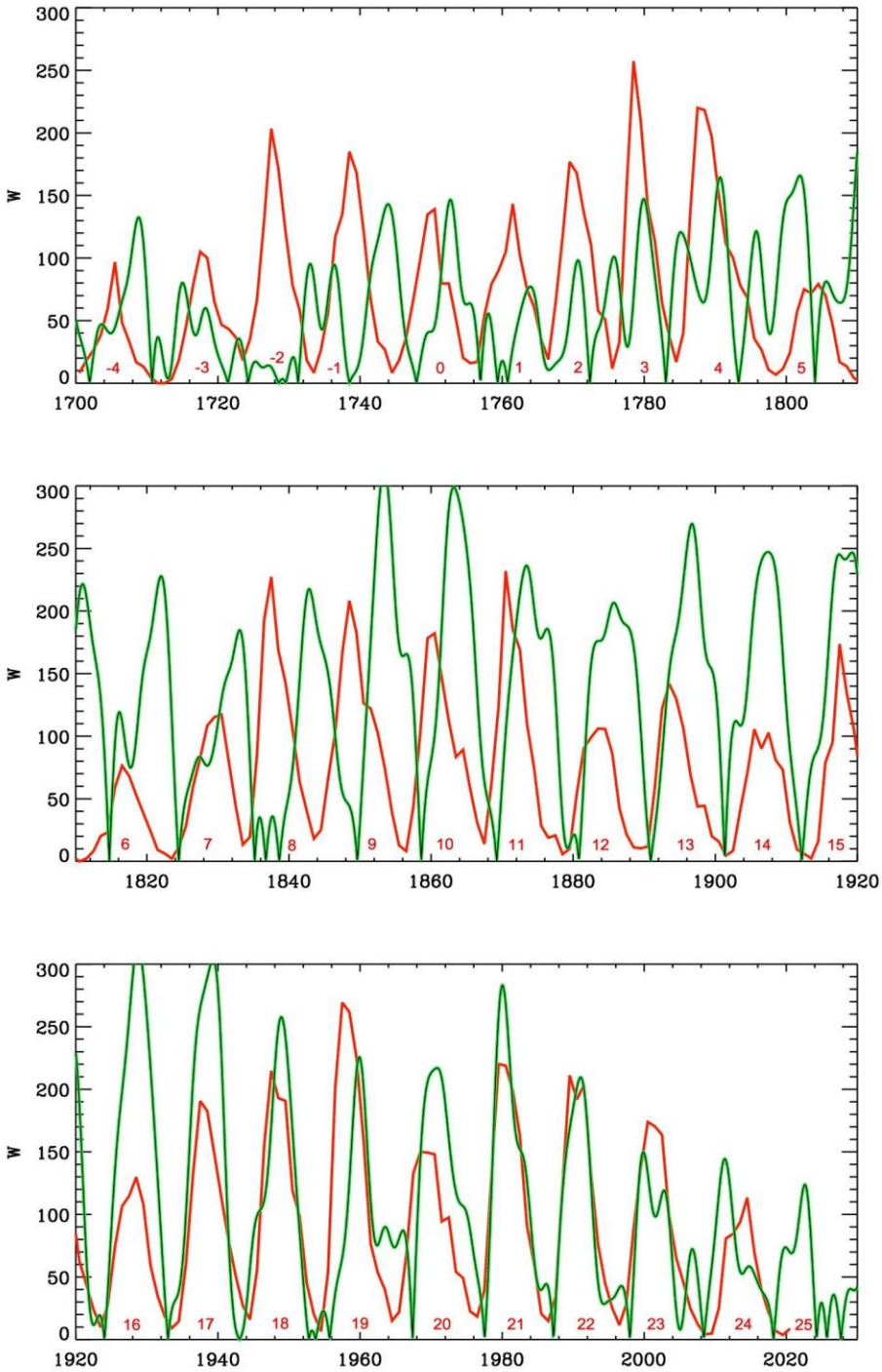

Fig.5. Comparison of the modulus summary curve (green line) with all the sunspot indices in all the sunspot cycles from 1700 (red line). Courtesy of Zharkova et al, 2023.

The summary curve for dipole magnetic sources gives 67% correlation with sunspot activity index including all the waves, not only dipole ones. Popova et al. (2018) has demonstrated that by adding to the summary curve the pair of magnetic waves induced by quadruple magnetic sources which are also found to be responsible for flaring activity on the Sun, at least, in soft X-ray emission (Zharkova and Shepherd, 2022) allows to improve this correlation with sunspot index to about 80%.

Hence, the summary curve of two largest eigen vectors, or two dynamo magnetic waves, produced by solar dipole magnetic sources, defines the appearance of the magnetic field on the solar surface. This summary curve revealed the occurrence of grand solar cycles with duration of 330-380 years separated by grand solar minima fitting numerous observations of the solar activity (Zharkova et al, 2015, 2018, 2023).

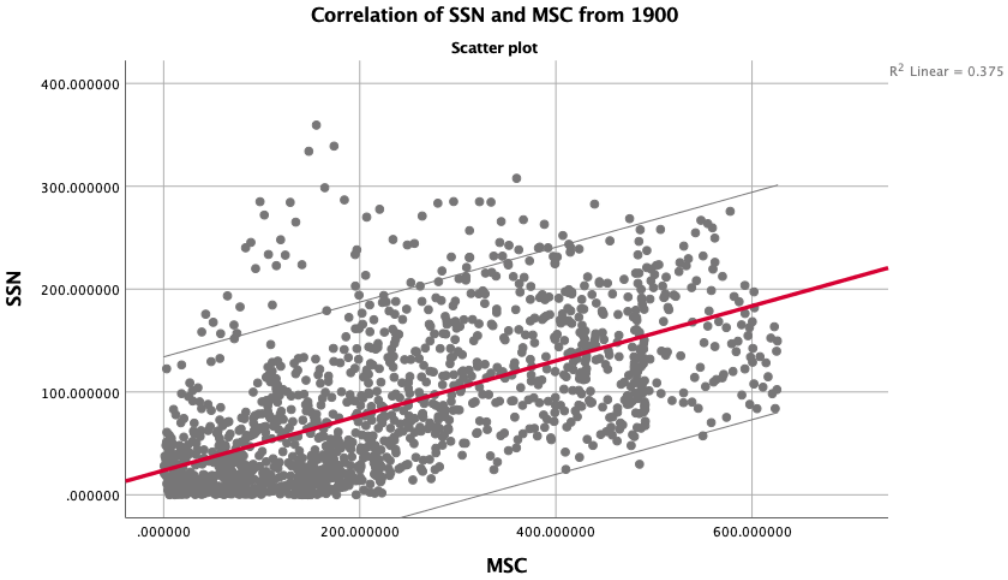

Fig.6. A scatter plot of the correlation of the modulus summary curve with the averaged sunspot numbers SSN measured from 1900 until 2022 years.

4. Grand solar cycles (GSCs) and grand solar minima (GSMs)

The derived analytical formula for the two principal components of SBMF, or dynamo magnetic waves, allows one to present the *summary curve* for years 1200-3200 shown in Fig.7 (Zharkova et al, 2015). This expanded *summary curve* reveals the distinct periodic variations of the 11-years cycle amplitudes with the envelope period of 330–380 years, or Grand Solar Cycles (GSCs). These GSCs are separated by Grand Solar Minima (GSMs), lasting from 3 to 7 solar cycles when these amplitudes of 11 years cycles become rather small, similar to those reported during Maunder, Wolf, Oort GSMs in AD or Homeric GSM in BC and many other Grand Solar Minima occurred in the past or to occur the future (Zharkova et al, 2018b).

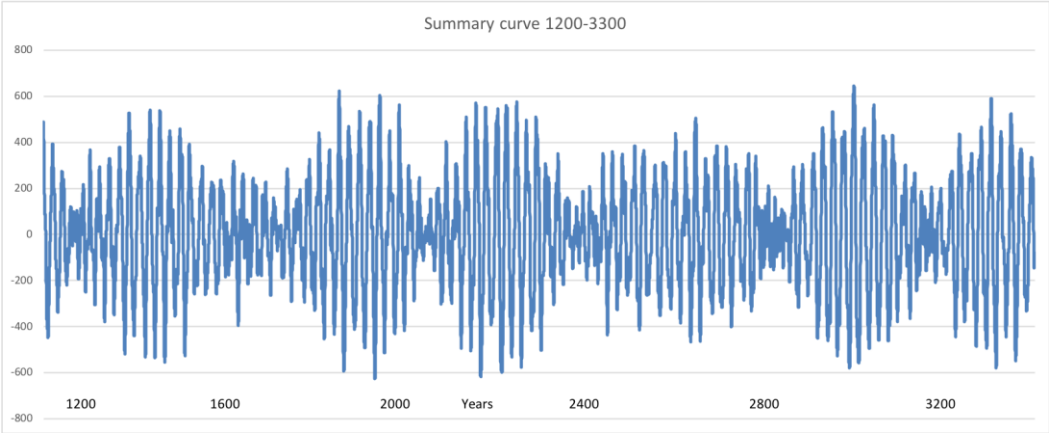

Fig.7. Summary curve of two PCs expanded to years 1200-3200 (Zharkova et al, 2015, Zharkova, 2020) revealing grand solar cycles (GSCs) of 330-380 years and grand solar minima (GSMs) between them.

Most importantly, the *summary curve* has timely uncovered the fact that there is the modern Grand Solar Minimum to occur in cycles 25–27, or in 2020–2053 (Zharkova et al, 2015), which can cause a substantial reduction (up to 1.0C) of the terrestrial temperature (Lean et al, 1995, Zharkova, 2020) like it has occurred during Maunder Minimum in the 17th century. The occurrence of the modern GSM in cycles 25-27 was also confirmed by Bayesian representation of averaged sunspot numbers SSN by Velasco Herrera et al (2021) considering the most accurate part of SSN after 1900 (Svalgaard and Schatten, 2016).

The expansion of this *summary curve* of two PCs, or EVs, up to 3000 years backwards shown that the *summary curve* reveals many Grand Solar Minima in the past, like named ones: Maunder, Wolf, Oort in last two millennia plus also the Homeric minimum about 800 years in the millennium BC (see Fig.8) and (Zharkova et al, 2018a,b).

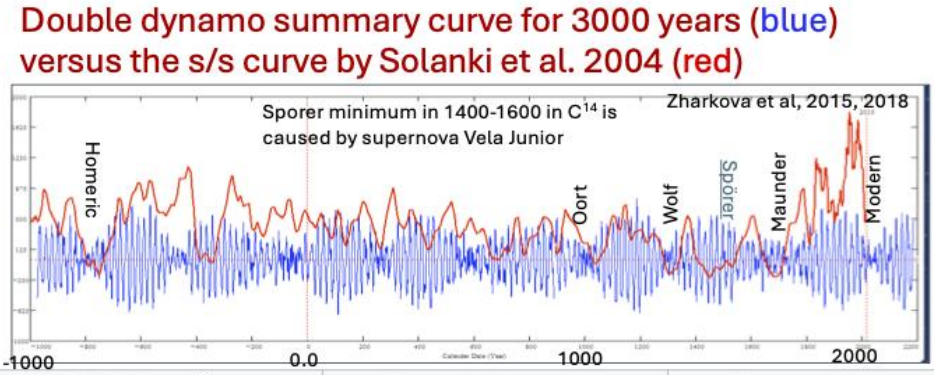

Homeric GS minimum[13]	-800 BC	-550 BC
Oort GS minimum	1040 AD	1080 AD
Medieval GS maximum	1100	1250
Wolf GS minimum	1280	1350
Spörer Minimum	1450	1550 Caused by SN Vela Junior
Maunder GS Minimum	1645	1715
Modern GSM	2020	2053

Fig.8. Solar activity index for 3200 years presented by the summary curve of eigen vectors (blue line) (Zharkova et al, 2015) versus the solar activity index derived from the isotopes C14 abundances in the terrestrial biomass (red line) (Solanki et al., 2004).

The most GSMs in the Holocene were nicely recovered by the *summary curve* index shown in Fig.8 (Zharkova et al, 2018a) besides Spoerer's solar minimum (Zharkova et al., 2017, 2018a) that is likely related to the increase Galactic Cosmic Rays (GCRs) background intensity on Earth in the times of Spoerer minimum. This increase was strongly affected by the explosion of supernova Vela Junior at the close distance of 650 light years from the Sun which significantly increased the GCR background radiation used in time dating leading to the potential errors in calculating the timing from C14 isotopes by up to 300 years (Zharkova et al, 2017). In fact, Zharkova et al, 2017 shows that the visual observations of large sunspots by Chinese astronomers, Aurora Borealis large intensities, the ice areas reduction in Greenland, the temperature variations and the increase of viral diseases on Earth during this period, all indicate to a maximum of solar activity and not the minimum as it was claimed.

5. Two natural frequencies of SBMF versus a dynamo model

In order to understand the natural frequencies of the *summary curve* derived from the full disk solar magnetograms, Parker's two layers αΩ-dynamo model was utilised for the dipole magnetic sources of the Sun producing dynamo magnetic waves for both poloidal and toroidal components in the two layers (inner and outer) with the opposite directions of meridional circulation

(Zharkova et al, 2015). One layer is assumed located deeply in the solar interior near the bottom of convective zone and another layer appearing beneath the solar surface. The original *summary curve* with the Grand Solar Cycles of SBMF (Zharkova et al, 2015) shown in Fig.7 was fit pretty closely all GSCs and GSMs by Parker's two layers αΩ-dynamo model (Parker, 1993, Popova 2018) for both, poloidal and toroidal magnetic field components using very reasonable parameters of the solar interior in both layers with the only difference in meridional circulation velocities of about 1 km/s leading to the required phase shift between the two magnetic waves (Zharkova et al., 2023).

6. Effects of grand solar minimum on the terrestrial temperature

A significant reduction of the solar activity during a grand solar minimum reflected in the reduction of the amplitude of the summary curve of two eigen vectors or a reduction in an averaged sunspot number leads to a noticeable (about 3 W/m^2) reduction of the solar radiation sent to Earth (Lean et al, 1995, Steinhilber et al, 2012). This reduction of solar radiation is shown to lead to a decrease the terrestrial temperature by 1.0 C-1.5 C over the whole Globe (Pfister, 1995; Shindell et al., 2001) as shown in Fig.9 for the Northern hemisphere for Maunder minimum, (1645-1710), the previous grand solar minimum in the 17th century. The temperature decrease is not similar in different parts of the Earth as shown by colour bars in Fig. 9.

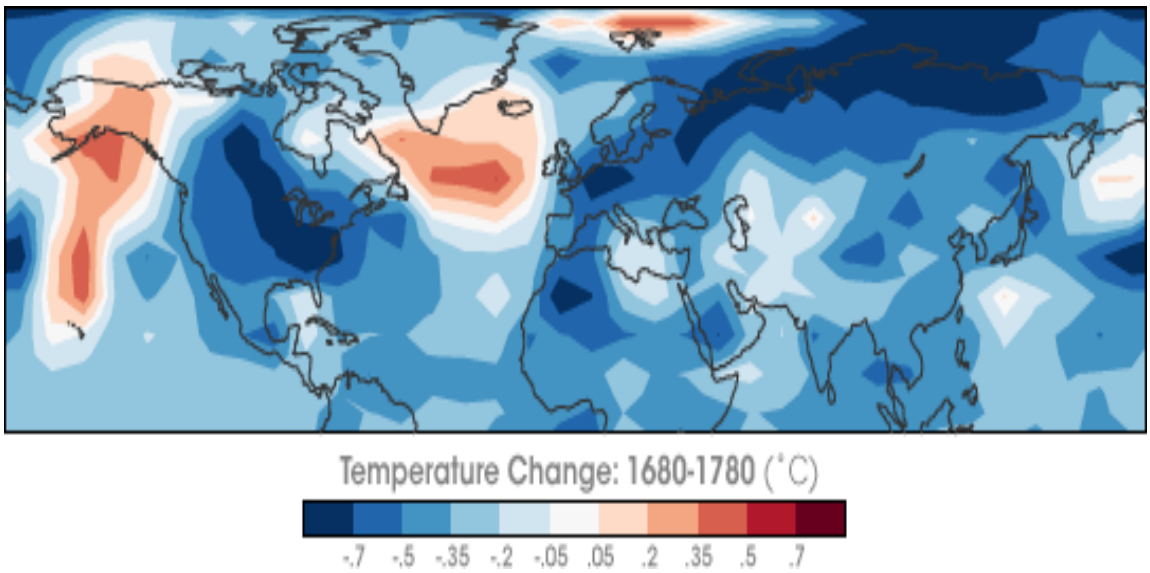

Fig.9. Annual change of the averaged surface temperature (in °C) in the northern hemisphere from 1780 to 1680 during the GCM. Courtesy of Shindell et al., 2001.

Shindell et al, 2001 used a version of General Circulation Model (GCM) of the Goddard Institute for Space Studies (GISS), which included a detailed representation of the stratosphere, and simulated the difference between the temperature measured in the GSM period and a century later, after the solar output became relatively high and stable. The model utilized a mixed-layer ocean, allowing sea surface temperatures (SSTs) to respond to radiative forcing, and has been shown to capture reasonably well the observed wintertime temperature variations induced by this GSM (Shindell et al, 1999). The GCM also included a parameterization of the response of ozone to solar irradiance, temperature, and circulation changes (Shindell et al, 1999), based on results for preindustrial conditions from their two-dimensional chemistry model (Shindell et al, 1998).

The simulations shown that the reduced Maunder Minimum irradiance leads to the increased

abundances of the upper stratospheric ozone that, in turn, leads to a decrease of the lower stratospheric ozone. These two processes produce a negative radiative forcing, e.g. the reduced solar irradiance during the Maunder Minimum causes a shift toward the low-index of AO/NAO (the Arctic Oscillation (AO) pattern or the North Atlantic Oscillation (NAO)) as demonstrated in Fig.10). These arctic jets led to Europe and Northern America to become unusually cold during the Maunder Minimum.

The surface temperature changes in November – February in Northern hemisphere show the alternating warm oceans and cold continents at the NH mid-latitudes (Fig. 9), with a maximum temperature decrease by 2.0-4.0C in winter. During December to February, even the surface temperature in the tropics and subtropics is found to cool by 0.4° to 0.5°C because of the reduced incoming radiation and the upper stratospheric ozone increase. Cooling in the tropical and subtropical upper troposphere is even more pronounced (0.8°C) because of cloud feedbacks, including an 0.5% decrease in high cloud cover induced by ozone through surface effects.

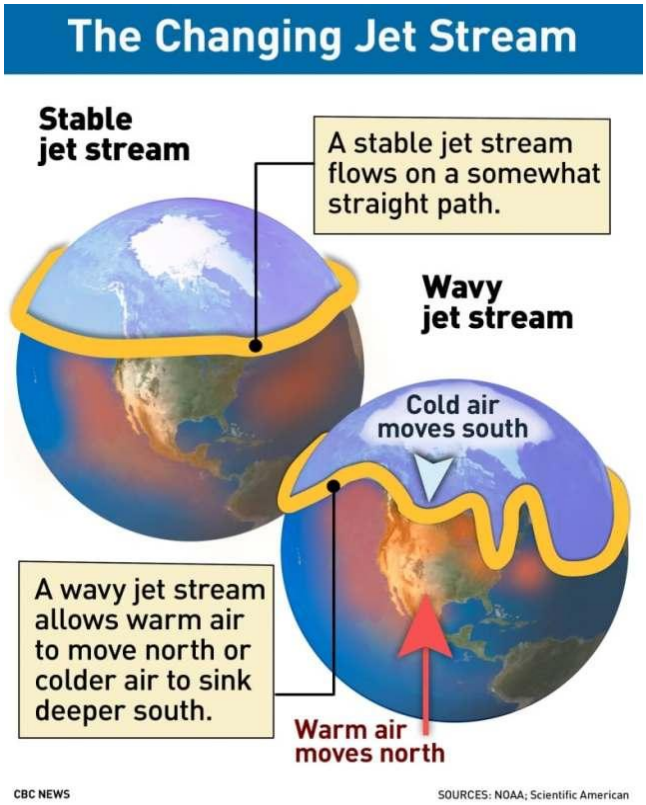

Fig. 10. Cartoon demonstrating formation of wavy jet wiggles in AO/NAO allowing the excursions of the arctic cold air into lower latitudes.

7. The signs of cold patches in the modern GSM

Currently, in January-February 2026 there are snows and frost all over the Northern hemisphere https://solargsm.com from the East (Japan, China) through Europe to the West (USA and Canada). The frost and snow reached subtropics in Florida and Caribbean (Cuba), there is also reported a cold weather in tropics (Singapore, Laos). There were the signs of cold in the Southern hemisphere as well like a frost and snow in Canberra on the 2 December 2026, the lowest January temperature -49.8 C in Antarctica, cold and wet weather in January in New Zealand. It shows that these arctic jets mentioned above are already making their ways to lower latitudes of each hemisphere including subtropics and tropics.

And all this cold is happenings while the sun just passed a maximum of cycle 25. Much more signs of cooling will be observed during the descending phase of cycle 25 and especially during a minimum between cycles 25 and 26 and 26 and 27. The next cycle 26 is predicted (Fig. 4) to have much less activity than other cycles. Moreover, it is shown (Vasilieva and Zharkova, 2023) that there is expected strong volcanic activity during cycle 26 that can contribute to further cooling of the terrestrial atmosphere. This puts into the focus the need of maximal reliable and continuous 24/7 energy resources required to heat people houses and food to feed humankind and animals.

8.Conclusions

In summary, it can be concluded that the modern grand solar minimum (2020-2053) predicted 10 years ago by Zharkova et al, 2015 has arrived and will progress as expected until the mid of century. There is the cold weather with huge frosts and snows recorded in January- February 2026 in the whole Northern hemisphere from the West to the East and from the North to the equator. The little ice age associated with the modern grand solar minimum is here, and the humankind needs to deal with it.

Each country needs more reliable and continuous energy resources helping humans keep their houses warm. All the governments need to find alternative resources to grow up or transport from the meat, vegetables, fruits and wheat/rye to supply food for population and animals.

In addition, let us remember that the GSM indicates a reduction of the solar background magnetic field (SBMF), which expands into the interplanetary space and reaches the planets. It means that this weakened interplanetary magnetic field gives all initiatives back to the planetary magnetic fields including the Earth magnetic field. This is the time to look more closely what is expected from the terrestrial pole swapping for the Earth, in general, and for the humankind, in particular.

Funding

The work was funded by the charity donations only.

Co-Editor: Stein Storlie Bergsmark

Acknowledgements

Acknowledgements for support of the publication to the charities of First Corporate Consultants Ltd., CiteEnergy Inc. and donations by the public.

References

Cameron, R. H.; Dikpati, M.; Brandenburg, A., 2017, "The Global Solar Dynamo", Space Science Reviews, ***210*** *(1–4):* 367–*395*

Hoeksema, J. T., 1984, *Structure and Evolution of the Large Scale Solar and Heliospheric Magnetic Fields*, STANFORD UNIVERSITY, 1984.Source: Dissertation Abstracts International, Volume: 45-06, Section: B, page: 1811.

Jolliffe, I. T. (2002). "Principal Component Analysis". Springer Series in Statistics. Berlin: Springer.

Lean JL, Beer J, Bradley R,. 1995, *Reconstruction of solar irradiance since 1610: Implications for climate change,* Geophys Res Lett., 22:3195–3198.

Parker, E. N. 1955, *Hydromagnetic Dynamo Models*, Astrophys. J. 122, 293

Parker, E. N., 1958, "*Dynamics of the Interplanetary Gas and Magnetic Fields.*", *The Astrophysical Journal*, **128**: 664
Parker E. N., 1993, *A Solar Dynamo Surface Wave at the Interface between Convection and Nonuniform Rotation*, Astrophys, J, 408, 707

*Popova E., Zharkova, V.V., Shepherd S.J. and Zharkov S. I., 2018, "On a role of quadruple component of magnetic field in defining solar activity in grand cycles", J. of Atmospheric and Solar-Terrestrial Physics. **176** (3):* 61–*68*C.

Pfister, C.,1995, *CLIMATE HISTORY AND THE MODERN WORLD*, 2 edn, Hubert H. Lamb, Routledge (London), 1995. 433pp.

D. T. Shindell, D. Rind, P. Lonergan, 1998, *Climate Change and the Middle Atmosphere. Part IV: Ozone Response to Doubled CO_2.*, J. Climate. 11/5, 895

D. T. Shindell, D. Rind, N. Balachandran, J. Lean, P. Lonergan, 1999, *Solar Cycle Variability, Ozone, and Climate*, Science 284, 305

D. T. Shindell, G. Schmidt, M. Mann, D. Rind, A.Waple, 2001, *Solar Forcing of Regional Climate Change During the Maunder Minimum*, Science 294, 2149-2152

*Shepherd, S.I.; Zharkov S.I.; Zharkova, V.V., 2014, "Prediction of solar activity from solar background magnetic field variations in cycles 21-23", Astrophysical Journal. **795** (46): 8*

*Smith, Edward J., 2001, "The heliospheric current sheet", Journal of Geophysical Research, **106** (A8): 15819–15831*

*Solanki, S. K.; Usoskin, I. G.; Kromer, B.; Schüssler, M.; Beer, J., 2004. "Unusual activity of the Sun during recent decades compared to the previous 11,000 years", Nature. **431** (7012):* 1084–*1087*

*Stix, M., 1976,. "Differential rotation and the solar dynamo", Astronomy and Astrophysics. **47** (2):* 243–*254*

*Svalgaard, Leif; Schatten, Kenneth H., 2016, "Reconstruction of the Sunspot Group Number: The Backbone Method', Solar Physics. **291** (9–10):* 2653–*2684*

Vasilieva I. and Zharkova V. *Links of Terrestrial Volcanic Eruptions to Solar Activity and Solar Magnetic Field,* 2023, **Global Journal of Science Frontier Research: A Physics and Space Science,** Volume 23 Issue 3 Version 1.0, 22-34

*Velasco Herrera, V. M.; Soon, W.; Legates, D. R., 2021, "Does Machine Learning reconstruct missing sunspots and forecast a new solar minimum?", Advances in Space Researc. **68** (3):* 1485–*1501*

Wolf, M., 1852, *On the Periodic Return of the Solar Spots,* Monthly Notices of the Royal Astronomical Society, Vol. 13, p.29

*Zharkov, S.; Gavryuseva E. Zharkova V., 2008, "The Observed Long- and Short-Term Phase Relation between the Toroidal and Poloidal Magnetic Fields in Cycle 23", Solar Phys.. **248** (2):* 339–*358.*

*Zharkova, V.V.; Shepherd, S.I.; Popova E.; Zharkov S.I. (2015), Heartbeat of the Sun from Principal Component Analysis and prediction of solar activity on a millennium timescale", Scientific Reports. **5**, 15689.*

Zharkova, V. V. ; Shepherd, S. J. ; Popova, E. ; Zharkov, S. I., 2017, "Reinforcing the double dynamo model with solar-terrestrial activity in the past three millennia", arXiv:1705.04482: 55

*Zharkova, V.V., Shepherd, S.J., Popova E., Zharkova, S.I., 2018a, "Reinforcing a Double Dynamo Model with Solar-Terrestrial Activity in the Past Three Millennia", Space Weather of the Heliosphere: Processes and Forecasts, Proceedings of the IAU Symposium. **335** (3):* 211*–215.*

*Zharkova, V.V., Shepherd, S.J., Popova E., Zharkova, S.I., 2018b, "Reply to comment by Usoskin (2017) on the paper "On a role of quadruple component of magnetic field in defining solar activity in grand cycle", J. of Atmospheric and Solar-Terrestrial Physics. **176** (3):* 72*–82*

Zharkova, V.V., 2020, "Modern Grand Solar Minimum will lead to terrestrial cooling", Temperature. 7 (3): 217*–222*

*Zharkova, V.V.; Shepherd, S.I., 2022, "Eigen vectors of solar magnetic field in cycles 21-24 and their links to solar activity indices", Monthly Notices of the Royal Astronomical Society. **512** (4):* 5085*–5099.*

*Zharkova, V.V.; Vasilieva I., Popova E., Shepherd, S.I., 2023, "Comparison of solar activity proxies: eigenvectors versus averaged sunspot numbers", Monthly Notices of the Royal Astronomical Society. **521** (4):* 6247*–6265*